Published OnlineFirst August 8, 2019; DOI: 10.1158/1535-7163.MCT-19-0115

Small Molecule Therapeutics

Molecular Cancer Therapeutics

A Novel Therapeutic Induces DEPTOR Degradation in Multiple Myeloma Cells with Resulting Tumor Cytotoxicity

Mario I. Vega[1], Yijiang Shi[1], Patrick Frost[1], Sara Huerta-Yepez[2,3], Gabriela Antonio-Andres[2,3], Rogelio Hernandez-Pando[4], Jihye Lee[5], Michael E. Jung[6,7], Joseph F. Gera[1,7], and Alan Lichtenstein[1,7]

Abstract

Prior work indicates DEPTOR expression in multiple myeloma cells could be a therapeutic target. DEPTOR binds to mTOR via its PDZ domain and inhibits mTOR kinase activity. We previously identified a drug, which prevented mTOR–DEPTOR binding (NSC126405) and induced multiple myeloma cytotoxicity. We now report on a related therapeutic, drug 3g, which induces proteasomal degradation of DEPTOR. DEPTOR degradation followed drug 3g binding to its PDZ domain and was not due to caspase activation or enhanced mTOR phosphorylation of DEPTOR. Drug 3g enhanced mTOR activity, and engaged the IRS-1/PI3K/AKT feedback loop with reduced phosphorylation of AKT on T308. Activation of TORC1, in part, mediated multiple myeloma cytotoxicity. Drug 3g was more effective than NSC126405 in preventing binding of recombinant DEPTOR to mTOR, preventing binding of DEPTOR to mTOR inside multiple myeloma cells, in activating mTOR and inducing apoptosis in multiple myeloma cells. *In vivo*, drug 3g injected daily abrogated DEPTOR expression in xenograft tumors and induced an antitumor effect although modest weight loss was seen. Every-other-day treatment, however, was equally effective without weight loss. Drug 3g also reduced DEPTOR expression in normal tissues. Although no potential toxicity was identified in hematopoietic or hepatic function, moderate cardiac enlargement and glomerular mesangial hypertrophy was seen. DEPTOR protected multiple myeloma cells against bortezomib suggesting anti-DEPTOR drugs could synergize with proteasome inhibitors (PI). Indeed, combinations of drug NSC126405 + bortezomib were synergistic. In contrast, drug 3g was not and was even antagonistic. This antagonism was probably due to prevention of proteasomal DEPTOR degradation.

Introduction

Overexpression of the mTOR inhibitor DEPTOR occurs specifically in multiple myeloma tumor cells (1). In addition, DEPTOR knockdown in multiple myeloma lines is cytotoxic (1, 2), suggesting DEPTOR could be a viable therapeutic target. In a previous study (3), we described a novel inhibitor, NSC126405, which bound to DEPTOR, prevented DEPTOR–mTOR binding and induced anti- multiple myeloma effects *in vitro* and *in vivo*. We now describe the molecular and anti- multiple myeloma effects of a chemically related compound which has the remarkable ability of inducing rapid proteasomal degradation of DEPTOR.

Materials and Methods

Cell lines, plasmids, transfections

All lines were obtained from ATCC. shRNAs targeting raptor and DEPTOR were described previously (3). The 13A mutant DEPTOR construct was a kind gift from Timothy Peterson (1). Lentiviral transduction of MM cell lines was as described (4).

Primary cells

As described previously (3), primary cells were purified from marrow by negative selection using the RosettesSep antibody mixture method. Purity was >99% plasma cells.

Binding between recombinant DEPTOR and mTOR

Beads containing anti-FLAG antibody were purchased from Sigma (Catalog No. A2220) and bound to FLAG-tagged mTOR as described (5). The pull-down assay exploiting these beads was described previously (5). In short, purified GST-DEPTOR was pretreated with increasing concentrations of drug NSC126405, or drug 3g for 1 hour at 4°C and subsequently added to mTOR-FLAG beads and then incubated overnight at 4°C. Incubated beads were washed and immunoblotted using anti-GST or anti-FLAG. The immunoblots were quantified by densitometry ($n = 3$) and the amount of GST-DEPTOR/FLAG-mTOR was calculated.

[1]Hematology-Oncology, VA West LA-UCLA Medical Center, Los Angeles, California. [2]Hospital Infantil de Mexico Federico Gomez, Mexico City, Mexico. [3]Pathology & Laboratory Medicine, UCLA Medical School, Los Angeles, California. [4]Patologia Experimental, Instituto Nacional de Ciencas Medicas, CDMX, Mexico. [5]Gachon University, Incheon, Korea. [6]Department of Chemistry & Biochemistry, University of California, Los Angeles, California. [7]Jonsson Cancer Center, University of California, Los Angeles, California.

Note: Supplementary data for this article are available at Molecular Cancer Therapeutics Online (http://mct.aacrjournals.org/).

Corresponding Author: Alan Lichtenstein, University of California Los Angeles, 11301 Wilshire Blvd, Bldg 304, Room E1-115, Los Angeles, CA 90073. Phone 310-478-3711, ext. 40021; Fax: 310-268-4508; E-mail: alan.lichtenstein@med.va.gov

Mol Cancer Ther 2019;18:1822–31

doi: 10.1158/1535-7163.MCT-19-0115

Published OnlineFirst August 8, 2019; DOI: 10.1158/1535-7163.MCT-19-0115

Photo-cross-linking assay

Photo-cross-linked NSC126405 or 3g were prepared as described previously (6). Purified GST-tagged native or truncated DEPTOR proteins were added to 20 μL of drug cross-linked or control non-cross-linked beads. After incubating at 4°C for 24 hours, the beads were washed 3 times and bound proteins eluted in 10% SDS-PAGE buffer at 100°C for 5 minutes. The eluted proteins were resolved by SDS-PAGE and immunoblotted using anti-GST antibodies.

Xenograft experiments

As described previously (3), 8226 cells were injected subcutaneously into NOD/SCID mice and randomized to receive intraperitoneal injections of drug or vehicle (DMSO). Tumor size was measured daily during treatment. Treatment groups compared drug 3g at 5 mg/kg/day versus DMSO or, separately, drug 3g at 20 mg/kg/day versus DMSO. A separate group of mice were treated every other day. In addition, a bone marrow-based model was used where luciferase-expressing 8226 multiple myeloma cells (10^7/mouse) were injected intravenously into NOG mice. After engraftment was confirmed by a positive bioluminescence signal, mice were randomized into controls (DMSO injections) or drug 3g–treated groups (5 or 10 mg/kg daily i.p. ×20 days). Total bioluminescence was assessed as described previously (7). An additional experiment utilized immunocompetent tumor-free Balb/C mice injected intraperitoneally daily with a range of concentrations of drug 3g versus DMSO. After 21 days, mice were sacrificed and blood and organs retrieved for analysis.

Immunohistochemistry

Four-micrometer-thick sections of tissue blocks were cut and stained using the Vectastain Elite ABC HRP Kit (Vector) in a 2-step IHC technique as described previously (8, 9). Antigen retrieval was performed and slides were incubated with primary antibody against phosphorylated p70 (1:500 dilution) from Invitrogen or DEPTOR (1:750 dilution) from Novus.

Digital analysis

As described previously (8, 9), the IHC-stained sections were digitized using an Aperio ScanScope CS, which obtains 40× digital images with high resolution (0.45 μm/pixel). Images were reviewed using an ImageScope (Aperio) to quantify marker expression. An algorithm was developed for each tissue to quantify total protein expression (positive pixel count algorithm). The ImageScope allowed the setting of a threshold for color saturation as well as upper and lower limits for intensities of weak-, moderately-, and strong-positive pixels. The Aperio apparatus scans the entire DEPTOR-stained tissue section, corresponding to a total area of 10,000 μm^2. Data are presented as total density expression/μm^2 calculated from a combination of intensity and percent positive pixels. For each tissue assessed, 4 slides are analyzed (1 for each mouse). The data in Fig. 5B are expressed as mean ± SE, $n = 4$ (slides/organ).

Surface plasmon resonance

Drug 3g binding to recombinant DEPTOR was also assessed in a surface plasmon resonance (SPR) assay as described previously (3). Briefly, recombinant DEPTOR was immobilized on a BIAcore CM5 sensor chip and analyte solution was prepared in a standard BIAcore buffer. Binding was measured by observing the change in the SPR angle as 30 μL of analyte flowed over the sample for 3 minutes at 10 μL/min. K_D values were calculated with BIAcore's BIAevaluation software, version 4.1.

Statistical analysis

To assess growth curves, tumor volumes were calculated as mean ± SEM. Repeated-measures analysis of variance was used to determine statistical significance of differences between the growth of tumors. Combinatorial indices were calculated as described previously (10) using the Calcusyn software Version 1.1.1 (Biosoft). For all other analyses, the Student *t* test was used to determine significance.

Results

Compound 3g is more effective than NSC126405

Drug NSC126405 was initially selected from a 2-yeast hybrid screen designed to identify inhibitors of mTOR–DEPTOR binding. This small inhibitor is cytotoxic to high DEPTOR-expressing multiple myeloma cell lines with an IC_{50} in the 1 to 4 μmol/L range (3). We then synthesized 53 chemically modified derivatives in an attempt to enhance anti-multiple myeloma effects. Of these agents, compound 3g was found to have the greatest therapeutic window as its IC_{50} against the 8226 multiple myeloma cell line decreased to 0.17 μmol/L without any increased cytotoxicity against normal PBLs. Compound 3g is an N-aryl derivative of NSC126405 (Fig. 1A) with a 3-trifluoromethylphenyl substituent. Its synthesis is described in ref. 11. Fig. 1B demonstrates the enhanced ability of compound 3g to induce cytotoxicity to 8226 multiple myeloma cells, which overexpress DEPTOR as a result of a MAF-translocation as DEPTOR is a transcriptional target of MAF (1). The IC_{50} for 8226 cells in the MTT assays shown for drug 3g is approximately 0.12 μmol/L whereas NSC126405 had no significant effect at concentrations of 0.5 μmol/L or below (MTT IC_{50} for NSC126405 against 8226 cells is approximately 1.2 μmol/L; ref. 3). Compound 3g is also more effective than NSC126405 against OPM-2 and H929 multiple myeloma lines with high DEPTOR expression (Fig. 1B). Apoptosis assays (Fig. 1C) similarly demonstrate enhanced efficacy of compound 3g. As stated above, drug 3g has no significant effect on viability of normal PBLs. In addition, the drug has no adverse effect on normal hematopoietic colony formation or nonmyeloma cell lines (Supplementary Fig. S1).

DEPTOR knockdown-induced multiple myeloma cytotoxicity is prevented by TORC1 paralysis (1, 4). To test if a similar effect on TORC1 activity regulates drug 3g's anti-multiple myeloma efficacy, we paralyzed TORC1 activity in 8226 cells by knocking down RAPTOR (Fig. 1D). This prevented activation of TORC1, monitored by p70 phosphorylation (Fig. 1D, bottom). TORC1-paralyzed multiple myeloma cells were significantly protected from drug 3g in terms of MTT cytotoxicity and apoptosis (Fig. 1E). These data confirm that acute activation of mTORC1 plays a role in drug 3g-mediated multiple myeloma cell cytotoxicity. We also noted that drug 3g exposure resulted in loss of DEPTOR expression (Fig. 1D). This is further studied later.

Co-immunoprecipitation experiments confirmed the ability of NSC126405 to inhibit mTOR–DEPTOR binding within multiple myeloma cells (3). As expected, Supplementary Fig. S2A demonstrates the ability of compound 3g to also prevent binding of DEPTOR to mTOR in 8226 cells but at a lower concentration of drug. As shown, 1 μmol/L of NSC126405 was effective in preventing binding but 0.5 μmol/L had no effect (Supplementary

Published OnlineFirst August 8, 2019; DOI: 10.1158/1535-7163.MCT-19-0115

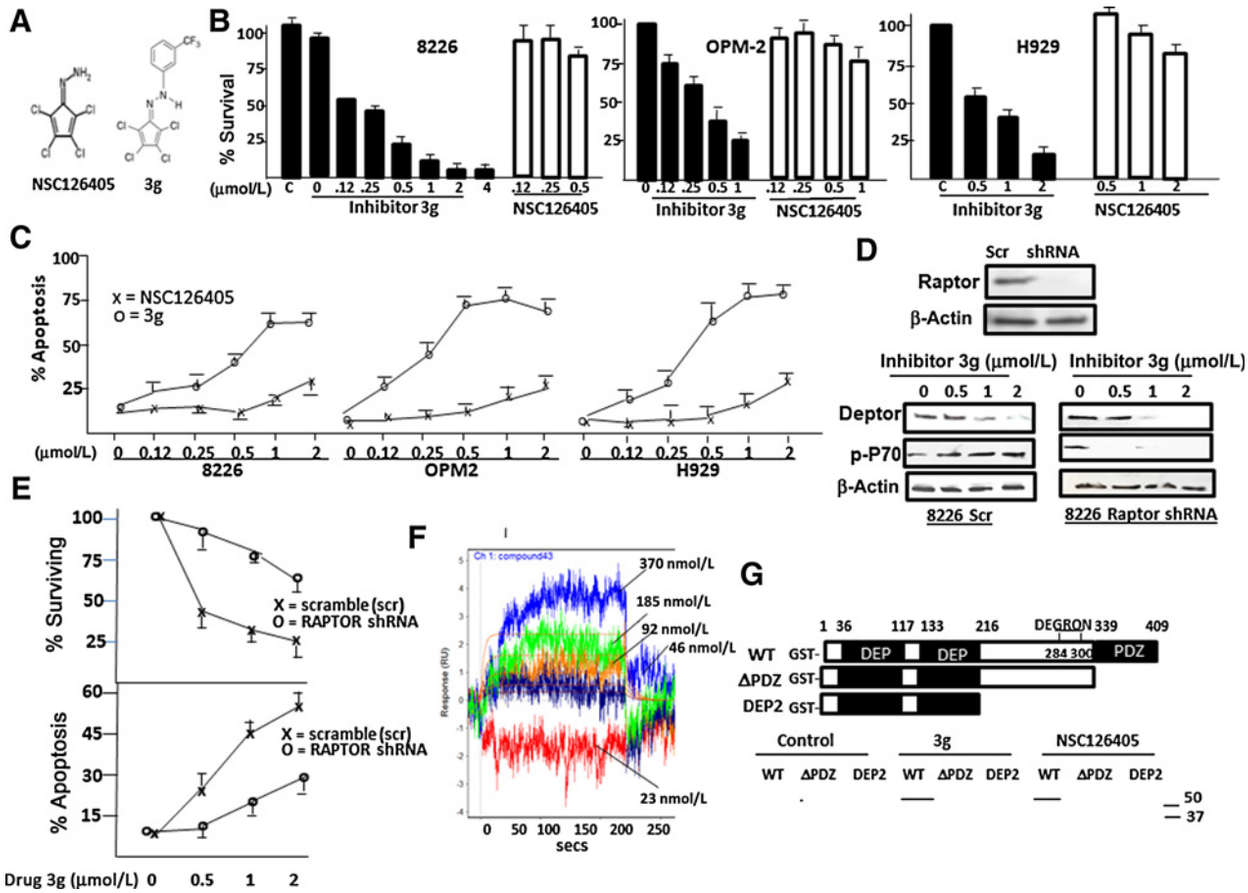

Figure 1.

Cytotoxic effects of DEPTOR inhibitors. **A,** Structures of NSC126405 and 3g. **B,** % survival (MTT assays) at increasing concentrations of inhibitors (48 hours assay) for 3 multiple myeloma cell lines. Results are mean ± SD, $n = 5$. **C,** % apoptosis induced at 48 hours (X = NSC126405; 0 = 3g), mean ± SD, $n = 3$. **D,** Immunoblot of control 8226 cells (Scr = scrambled sequence shRNA) or RAPTOR-silenced 8226 cells (top) and immunoblot of control or RAPTOR-silenced cells incubated with drug 3g for 8 hours (bottom). **E,** MTT (top) or apoptosis (bottom) assays in both cell lines after 48 hours. Means ± SD, $n = 3$. **F,** Surface plasmon resonance assay (see Materials and Methods) where increasing concentrations of 3G-containing analyte is passed over immobilized recombinant DEPTOR. **G,** top, structure of 3 recombinant DEPTOR proteins used in drug binding assay (see Materials and Methods); bottom, binding of 3g or NSC126405 to WT or truncated DEPTOR proteins.

Fig. S2A, top). In contrast, 0.5 μmol/L of drug 3g prevented DEPTOR–mTOR binding in multiple myeloma cells (Supplementary Fig. S2A, bottom). Because DEPTOR binding to mTOR results in depressed mTOR activity (1), drugs that prevent binding should enhance mTOR activity. As expected, inhibitor 3g activates TORC1 activity demonstrated by increased phosphorylation of the TORC1 substrates p70S6K and 4EBP-1 (Supplementary Fig. S2B and S2C). Notably, enhanced activity occurred at lower concentrations of 3g (0.25 μmol/L for p70 and 4EBP-1 phosphorylation) compared with NSC126405. Enhanced phosphorylation of the p70S6K substrate, S6, also occurred at lower concentrations of inhibitor 3g (Supplementary Fig. S2C). An additional effect of NSC126405 is upregulated p21 expression, mediated by a TORC1-dependent decreased expression of p21-targeting miRNAs (4). Supplementary Fig. S2D demonstrates the ability of inhibitor 3g to upregulate p21 expression at lower concentrations versus NSC126405. In a pull-down assay (Supplementary Fig. S2E), drug 3g was also more effective than NSC126405 in preventing binding of recombinant DEPTOR to mTOR (IC_{50} of 1 μmol/L vs. 10.5 μmol/L for drug NSC126405).

DEPTOR knockdown, by upregulating mTORC1/p70S6K activity, results in phosphorylation of IRS-1 (12, 13) and subsequent feedback inhibition of PI3K/PDK1-mediated phosphorylation of AKT on T308. Prior work (3) with drug NSC126405 failed to demonstrate engagement of the negative feedback pathway. This is again demonstrated in the bottom panels of Supplementary Fig. S2F. However, Supplementary Fig. S2F (top) demonstrates that the feedback pathway is clearly engaged by exposure to drug 3g with decreased phosphorylation of AKT (T308) in 8226 and OPM-2 multiple myeloma cells. Although T308 phosphorylation is diminished by drug 3g, AKT S473 phosphorylation is enhanced, presumably due to TORC2 activation resulting from relieving DEPTOR suppression of mTOR. The increase in SGK phosphorylation (Supplementary Fig. S2F, top), an AKT substrate, suggests that the resulting effect of drug 3g on AKT kinase activity is moderate activation. It is remarkable that, in spite of

Published OnlineFirst August 8, 2019; DOI: 10.1158/1535-7163.MCT-19-0115

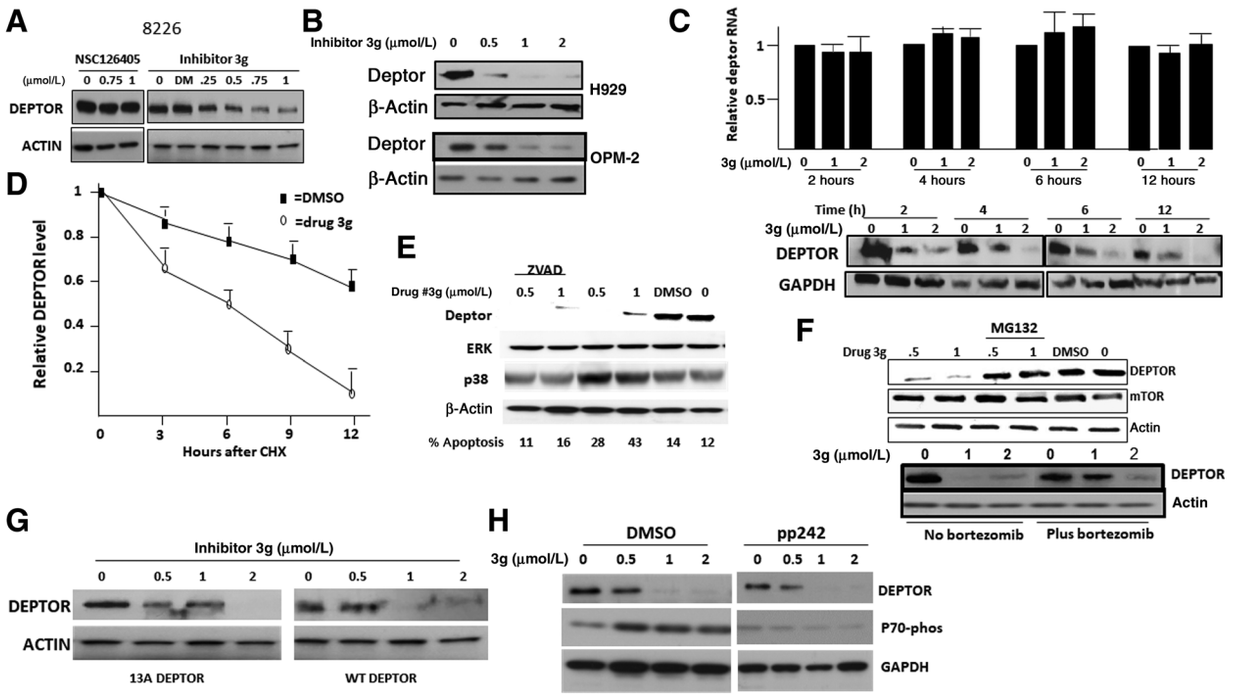

Figure 2.

Drug 3g induces DEPTOR degradation. **A** and **B,** Immunoblot of 8226, H929, or OPM-2 cells after 6-hour incubation with NSC126405 or 3g. **C,** 8226 cells incubated with 0, 1, or 2 μmol/L of 3g for 2, 4, 6, or 12 hours after which cells assayed for DEPTOR RNA (top, mean ± SD, $n = 3$) or DEPTOR protein (bottom). **D,** Pulse chase (8226 cells) experiment utilizing cycloheximide (CHX) comparing DMSO)- or 3g-treated cells. Results are means ± SD, $n = 3$. **E,** Immunoblot in 8226 cells after 4-hour treatment with DMSO or drug 3g at 0 (no DMSO), 0.5, or 1 μmol/L ± ZVAD used at 0.5 μmol/L. Below gel is % apoptosis assayed at 48 hours. **F,** Immunoblot after 3-hour treatment with DMSO or drug 3g at 0, 0.5, or 1 μmol/L ± MG132 used at 10 Um or ± bortezomib used at 10 nmol/L. **G,** Multiple myeloma cells transfected with either WT FLAG-DEPTOR or 13A FLAG-DEPTOR mutant, treated with drug 3g (4 hours) followed by immunoblot assay for FLAG. **H,** 8226 cells treated with drug 3g ± pp242 to inhibit mTOR, followed by immunoblot assay.

mTOR and AKT activation, drug 3g is still cytotoxic to high-DEPTOR-expressing multiple myeloma cell lines.

A prior study (3), with a surface plasmon resonance assay demonstrated that drug NSC126405 binds to recombinant DEPTOR. Additional experiments (Fig. 1F) likewise demonstrate binding of 3g to DEPTOR. Binding was rapid and reached an equilibrium plateau within seconds. In head-to-head experiments comparing dissociation constants, binding affinity of 3g to DEPTOR was not greater than NSC 126405 ($K_D = 330 \pm 20$ nmol/L vs. 230 ± 30 nmol/L for NSC126405, $n = 3$).

To identify where drug 3g binding occurs, we generated drug 3g or NSC126405 cross-linked affinity beads (6) and tested whether inhibitor-coupled beads bind to native or truncated GST-DEPTOR proteins (shown above in Fig. 1G). As shown below the schematic, wild-type (WT) DEPTOR bound to beads affinity-linked to both drugs but not to control beads (no drugs). Binding was lost in DEPTOR proteins that were missing the PDZ domain (ΔPDZ). These data suggest that both drugs similarly bind to the PDZ domain of DEPTOR.

Drug 3g induces DEPTOR degradation

The above molecular effects of drug 3g can be explained by inhibited binding of mTOR to DEPTOR and acute activation of mTOR. However, as mentioned above, compound 3g also results in loss of DEPTOR protein expression, which was not present in NSC126405-treated cells (Fig. 2A and B). Loss of DEPTOR protein occurs in a concentration-dependent fashion, and occurs within 2 hours as shown in Fig. 2C. Inhibition of DEPTOR protein expression is posttranscriptional (Fig. 2C) and associated with decreased protein survival/stability (Fig. 2D). To rule out a caspase-dependent degradation of DEPTOR, we cocultured cells with compound 3g ± ZVAD to inhibit caspases. As shown in Fig. 2E, although preventing apoptosis (results below gel), ZVAD could not prevent compound 3g-induced DEPTOR loss. Finally, as shown in Fig. 2F, the proteasome inhibitors (PI) MG132 and bortezomib significantly prevented DEPTOR loss, although 2 μmol/L of 3g could overcome the proteasomal inhibition due to 10 nmol/L bortezomib. These data suggest that, following DEPTOR binding of drug 3g, proteasomal degradation is stimulated.

DEPTOR protein turnover is physiologically regulated by mTOR-mediated phosphorylation of a degron located between the N-terminal DEP domains and the C-terminal PDZ domain (14–16). Although drug 3g results in activation of mTOR, its prevention of mTOR/DEPTOR binding suggests the enhanced proteasomal degradation of DEPTOR is not due to enhanced mTOR-dependent phosphorylation of the degron. Further support for this comes from preceding Fig. 1D, where drug 3g was comparably effective in causing DEPTOR protein loss in TORC1-paralyzed cells versus scramble (scr)-transfected control cells, arguing against a role for TORC1 kinase activity in DEPTOR degradation. We also addressed this possibility by using the

Published OnlineFirst August 8, 2019; DOI: 10.1158/1535-7163.MCT-19-0115

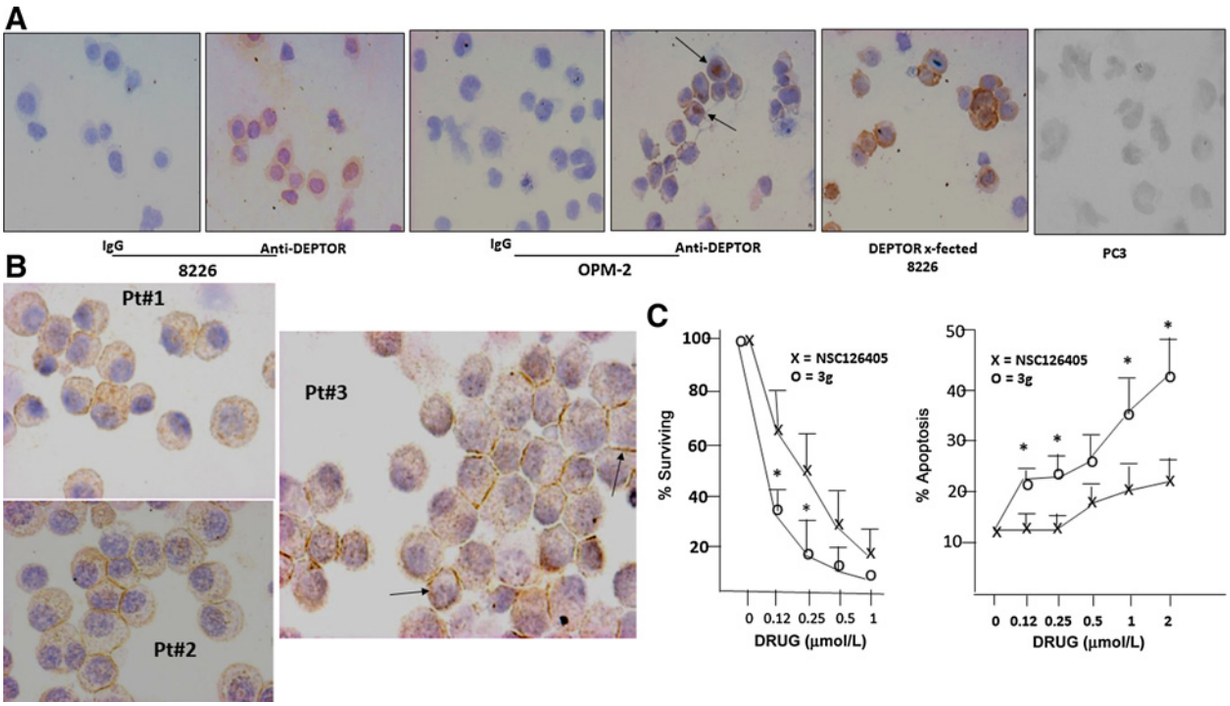

Figure 3.

Effects on primary multiple myeloma cells. **A,** Immunostaining of multiple myeloma (8226, OPM-2) or prostate cancer (PC3) cell lines with anti-DEPTOR antibody. Magnification ×40. **B,** Immunostaining of 3 primary multiple myeloma specimens from patients (magnification ×100). **C,** Primary multiple myeloma specimens ($n = 5$) treated with increasing concentrations of NSC126405 or 3g for 20 hours after which trypan blue staining and counting (% surviving, left) or apoptosis (right) assayed. Results are mean ± SD, $n = 5$. *, significantly ($P < 0.05$) different from NSC126405.

13A mutant version of DEPTOR which is rendered resistant to mTOR-dependent phosphorylation (1). As shown in Fig. 2G, 13A is also degraded by exposure to drug 3g. In addition, inhibition of mTOR kinase activity by co-incubation with the pp242 inhibitor (Fig. 2H) also did not prevent drug 3g-induced DEPTOR degradation.

Efficacy of drug 3g in primary multiple myeloma cells

To test effects in primary cells we compared drug 3g to NSC126405, after a 20-hour exposure. Five primary multiple myeloma samples were studied by CD138-isolation of bone marrow aspirate obtained from newly diagnosed patients (99% pure). Multiple myeloma cells from all 5 patients expressed DEPTOR protein as shown by IHC. As shown in Fig. 3A, our IHC antibody could detect DEPTOR expression in 8226, OPM-2, and DEPTOR-transfected 8226 cell lines but not in the PC3 prostate cancer cell line. Immunostaining appeared to be primarily cytoplasmic in 8226 cells while the staining pattern in some OPM-2 cells suggested nuclear staining (arrows). This is reminiscent of a recent report (17) that indicates intranuclear DEPTOR presence in some multiple myeloma cell lines. DEPTOR immunostaining in primary cells was intense and of a granular pattern (immunostaining of 3 of the 5 patients shown in Fig. 3B). There was additional immunostaining that appeared to be cell membrane-based (arrows). This cellular localization of DEPTOR is consistent with the known cytoplasmic granular and cell membrane localization of mTOR (18). Fig. 3C demonstrates the cytotoxic (cell survival, left) and apoptotic (right) effects of drug 3g against these 5 primary samples. At this early time point, viability of DMSO-treated control cells was excellent (>85%) with very minimal basal apoptosis. In drug-treated cultures, it was clear that compound 3g was more efficacious than NSC126405. None of our 5 primary samples were obtained from patients with MAF translocations, the subclass associated with the highest DEPTOR expression (1), suggesting these anti-DEPTOR drugs may be more broadly effective in multiple myeloma rather than just a specific small genetic subclass.

Effects of drug 3g in mice

To test if drug 3g had molecular effects *in vivo*, the 8226 cell line was injected sub-cutaneous (SQ) into immunodeficient mice and, when tumors were 500 mm^3, mice were treated with DMSO or drug 3g at 20 mg/kg by daily i.p. injection (4 mice/group). Tumors were excised after 4 days and analyzed. Treatment with 3g induced a rapid tumor cytoreductive effect (>50% reduction in tumor volume by 4 days; Supplementary Fig. S3). Fig. 4A demonstrates that treated tumors demonstrated loss of DEPTOR expression, corresponding enhanced p70 phosphorylation, decreased PCNA expression (proliferation marker), and increased AKT phosphorylation on S473. Thus, molecular effects of drug 3g used *in vivo* were similar to *in vitro* exposure. We next tested a longer treatment exposure (daily treatment x 9 days), comparing 5 mg/kg to DMSO or 20 mg/kg to DMSO. Treatment began when SQ tumors were approximately 200 to 300 mm^3. Although 5 mg/kg of drug 3g had only a modest slowing of tumor growth (although significant, $P < 0.05$; Supplementary Fig. S4A), 20 mg/kg once again induced a rapid antitumor effect and tumor rejection was complete in 3 of 8 mice (Fig. 4B). There was no tumor regrowth in

Published OnlineFirst August 8, 2019; DOI: 10.1158/1535-7163.MCT-19-0115

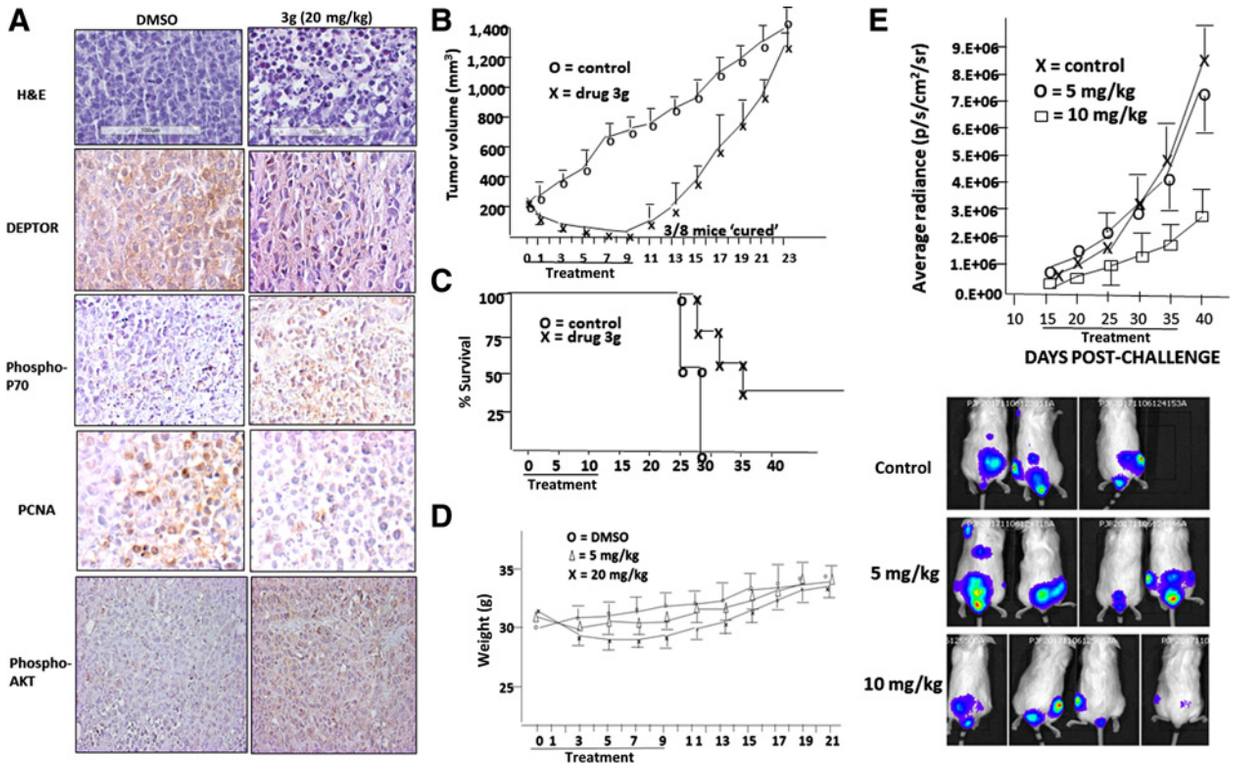

Figure 4.

Effects of 3g in mice. **A,** Immunostaining of tumors excised after 4 days of DMSO or 3g. Pictures are representative of all 4 murine tumors/group; magnification ×40. **B,** Tumor outgrowth in mice treated daily for 9 days with DMSO or 3g at 20 mg/kg. Results are mean ± SD tumor volume ($n = 8$ mice/group). **C,** Survival curve of experiment described in "**B**". **D,** Murine weights comparing DMSO injections to 5 or 20 mg/kg drug 3g administered intraperitoneally daily for 9 days. Results are mean ± SD. WTs of mice injected w/20 mg/kg were lower ($P < 0.05$) than control mice during the 9 days of treatment. **E,** Bioluminescence results in mice challenged intravenously with luciferase-expressing 8226 cells. When signal is first detected (day 15 postchallenge) mice randomized to receive DMSO (control $n = 3$) or drug 3g in intraperitoneally daily injections for 20 days at either 5 or 10 mg/kg ($n = 4$/group). Results are total bioluminescence (mean ± SD). Below graph are representative images of control mice and 5 or 10 mg/kg drug 3g-injected mice at day 40.

these 3 mice with up to 50 days of observation (Fig. 4C, survival curves). However, in the remaining 5 mice, tumor regrowth occurred after treatment cessation (Fig. 4B). Individual tumor growth curves are shown in Supplementary Fig. S4B. Fig. 4D demonstrates that at 20 mg/kg, drug 3g was associated with a small decrease in weight in this experiment (approximately 5% of body weight), which was rapidly corrected after treatment stopped. The lower dose of 5 mg/kg did not cause significant weight loss. In a separate experiment shown in Supplementary Fig. S4C and S4D, drug 3g was compared head-to-head with drug NSC126405. As shown, drug 3g was more efficacious in slowing tumor growth and prolonging survival, thus mirroring drug 3g's enhanced *in vitro* efficacy.

Drug 3g also demonstrated efficacy in a bone marrow-based murine model. Luciferase-expressing 8226 cells were injected intravenously and, when a bioluminescent signal was first detected in the skeleton of mice, treatment began with DMSO (control) or drug 3g. We used 5 and 10 mg/kg of drug 3g by daily i.p. injection as 20 mg/kg had previously induced some weight loss. Fig. 4E demonstrates a significant anti-tumor effect at 10 mg/kg in this model as compared with DMSO- or 5 mg/kg-treated cohorts. Neither 10 or 5 mg/kg of drug 3g had any impact on murine weight (Supplementary Fig. S4E).

Because daily treatment with 20 mg/kg of drug 3g resulted in some weight loss, we also tested if less frequent administration could be less problematic. SQ tumor-bearing mice were injected intraperitoneally with 20 mg/kg and tumors excised 24, 48, or 72 hours later for assessment of DEPTOR expression. As shown in Supplementary Fig. S5A, decreased expression was identified at 24 and 48 hours postinjection with re-expression seen by 72 hours. We, thus, treated tumor-bearing mice (8/group) with an every-other-day regimen with direct comparison to daily treatment. As shown in Supplementary Fig. S5B and S5C, the every-other-day regimen was equally effective and without weight loss. In fact, the absence of weight loss allowed retreatment with a secondary decrease in tumor growth.

To assess whether drug 3g affected normal tissues, we used normal tumor-free immunocompetent mice. Mice (4/group) were treated with increasing doses of drug 3g by daily intraperitoneal injection for up to 21 days. After 4 or 21 days of treatment, there was no significant effect on blood counts (Fig. 5A). Serum markers of hepatic and renal function were likewise unaffected (Supplementary Fig. S6). Nevertheless, after 21 days of drug 3g at 10 to 20 mg/kg, a loss of DEPTOR expression was detected in all organs tested. Fig. 5B demonstrates this in 10 mg/kg-injected mice by IHC assessment in kidney, liver, and heart (examples of IHC staining in Supplementary Fig. S7A). In addition, because IHC-identified expression of DEPTOR in heart tissue was relatively low, a confirmatory immunoblot (Supplementary Fig. S7B)

Published OnlineFirst August 8, 2019; DOI: 10.1158/1535-7163.MCT-19-0115

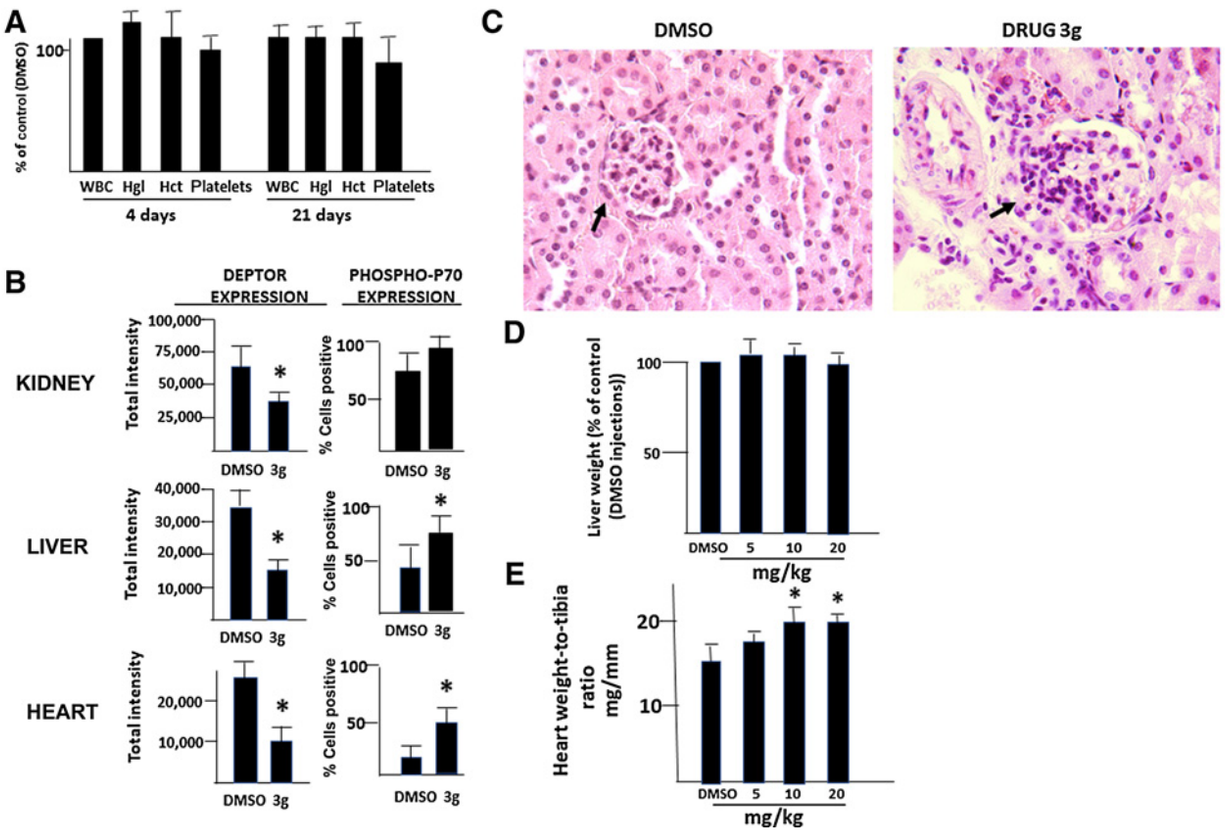

Figure 5.

Effects of 3g in immunocompetent mice. **A,** Blood counts [white blood cells (WBC)], hemoglobin (Hgl), hematocrit (HCT), and platelets after 4 or 21 days of daily drug 3g (20 mg/kg) compared with control (DMSO treatment, assumed to be 100%). Results are mean ± SD, $n = 4$. **B,** Semiquantitative assessment of DEPTOR or phosphorylated p70 expression (see Materials and Methods) in kidney, liver, or heart (mean ± SD, $n = 4$) after 21 days of DMSO or 3g treatment (10 mg/kg × 21 days) * = different from DMSO control, $P < 0.05$. **C,** Representative images of renal glomeruli (arrows) in DMSO-control-injected (left) or drug 3g-treated (10 mg/kg, right) mice (magnification ×400). **D,** liver weights expressed as % of control (DMSO), mean ± SD, $n = 4$. **E,** heart weight-to-tibia length ratios expressed as mg/mm, mean ± SD, $n = 4$; *, different than DMSO control, $P < 0.05$.

shows drug-induced loss of DEPTOR expression. There was a corresponding increase in percent of hepatic and cardiac cells staining positively for p70 phosphorylation in drug-treated mice (Fig. 5B). In contrast, although also slightly increased in renal tissue this did not reach statistical significance.

The alterations in DEPTOR expression and mTORC1 activity in normal tissues were of concern considering possible toxic effects. Specifically, prior reports detailed enhanced renal mesangial hypertrophy (19, 20) and cardiac hypertrophy (21) in mice with diminished DEPTOR expression and/or enhanced mTOR activity. Histologic analysis of renal sections in drug 3g-treated mice did identify a modest number of glomeruli (approx. 10%) with mesangial hypertrophy (example in Fig. 5C). In addition, heart weight/tibia length ratios were modestly increased in drug-treated mice (Fig. 5E). No alterations in liver weights were identified (Fig. 5D) and histologic examination of hepatic tissue was also unaltered in drug 3g-treated mice (Supplementary Fig. S8).

Effects on bortezomib sensitivity

Multiple myeloma cell lines transfected to overexpress DEPTOR or knockdown DEPTOR were exposed to increasing concentrations of bortezomib for 24 hours. As shown in Fig. 6A and B, DEPTOR knockdown with 2 independent shRNAs in high DEPTOR-expressing OPM-2 or 8226 multiple myeloma lines resulted in enhanced bortezomib-induced apoptosis. In contrast, ectopic overexpression of DEPTOR in the moderate DEPTOR-expressing U266 multiple myeloma line resulted in a decreased apoptotic response to bortezomib (Fig. 6C and D). Even the MAF-translocated 8226 line, when transfected to more markedly overexpress DEPTOR, demonstrated resistance to bortezomib (Fig. 6D). These results suggest an anti-DEPTOR drug could potentially synergize with bortezomib for enhanced anti-multiple myeloma effects. Indeed, when 8226 cells were treated with NSC126405 and bortezomib, synergy is identified (Fig. 6F), with a combinatorial index (CI) of 0.2. However, synergy is lost when bortezomib is combined with drug 3g (Fig. 6E) and, in fact, antagonism is seen with a CI of 1.8.

Discussion

In this report we describe a compound, 3g, which binds to DEPTOR and induces its proteasome-mediated degradation. Drug 3g binds to the PDZ domain of DEPTOR, which mediates its association with mTOR (1), and this specific PDZ binding

Published OnlineFirst August 8, 2019; DOI: 10.1158/1535-7163.MCT-19-0115

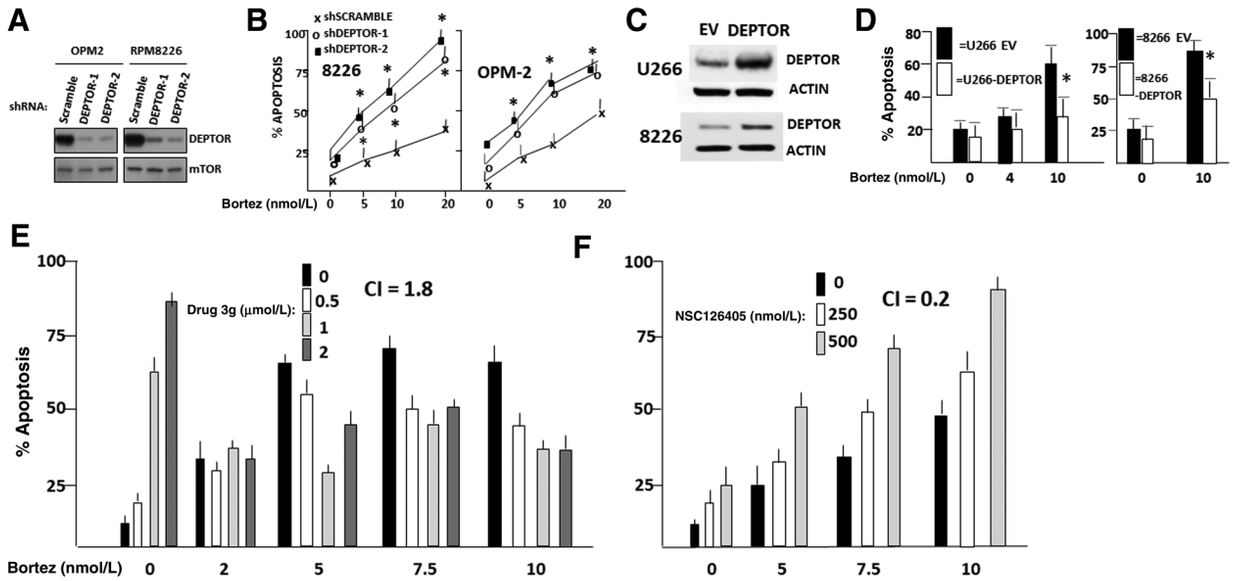

Figure 6.

Effects on bortezomib sensitivity. **A,** Immunoblot assay in cell lines transfected with shRNA to scrambled sequence or 2 separate sequences of DEPTOR. **B,** Apoptosis of cell lines of "**A**" when exposed to increasing concentrations (nmol/L) of bortezomib (Bortez) for 48 hours. Data are mean ± SD, $n = 3$. *, denotes apoptosis significantly greater ($P < 0.05$) than scramble-transfected line. **C,** Immunoblot assay of DEPTOR expression in U266 or 8226 multiple myeloma cell lines after transfection with empty vector (EV) or DEPTOR. **D,** % apoptosis of cell lines of "**C**" following 48-hour incubation with 0, 4, or 10 nmol/L bortezomib. Data are mean ± SD, $n = 3$; *, denotes significantly ($P < 0.05$) decreased apoptosis vs. EV-transfected control. **E** and **F,** % apoptosis (mean ± SD) of 8226 multiple myeloma cells treated for 48 hours with increasing concentrations of bortezomib ± NSC126405 or drug 3g. Combinatorial indices (CI) of combined treatment given above bars.

probably explains the ability of drug 3g to prevent DEPTOR/mTOR binding. Although the binding affinity of drug 3g is comparable to NSC126405, it is more effective at preventing association of recombinant DEPTOR to mTOR. In addition, its binding is qualitatively different, resulting in DEPTOR degradation, whereas NSC126405 does not alter DEPTOR protein levels. DEPTOR posttranslational modifications induced by binding of drug 3g (but not NSC126405) may mediate the proteasomal degradation and these are being investigated.

Drug 3g is also more effective than NSC126405 as an anti-multiple myeloma therapeutic. Its inhibitory effect on DEPTOR/mTOR binding inside multiple myeloma cells and subsequent acute mTORC activation occur at lower concentrations than NSC126405. The more effective inhibition of the proximal DEPTOR/mTOR binding may simply explain the heightened *in vitro* cytoreductive response of drug 3g. However, the drug 3g-induced degradation of DEPTOR could also participate in the greater anti-multiple myeloma effect if there are mTOR-independent progrowth/survival influences of DEPTOR in multiple myeloma cells. Indeed, recent reports (17, 22) indicate DEPTOR may protect against endoplasmic reticulum (ER) stress and maintain ER mass in an mTOR-independent fashion. As expected, drug 3g was more efficacious than NSC126405 *in vivo* in a SQ xenograft model.

Drug 3g induced loss of DEPTOR expression in normal tissues associated with TORC1 activation, eliciting concerns about toxicity. Whole-body DEPTOR knockout mice are phenotypically normal (23). However, there may be early compensatory mechanisms ameliorating DEPTOR loss in knockout mice that might not protect during drug-induced acute loss. Nevertheless, genetic deletion of DEPTOR specifically in liver in a strategy to limit compensatory mechanisms resulted in only moderate metabolic effects, primarily in fasting mice (23). In contrast, there was no alteration of liver weights nor change in lipid metabolism. Administration of drug 3g likewise had no effects on liver weight or on liver function tests. As suggested by Caron and colleagues (23), hepatic DEPTOR may be a secondary mTOR regulator, mostly coming into play during fasting whereas hepatic TSC1 is the master switch controlling mTORC activity.

An additional concern vis-à-vis toxicity related to renal effects. Activation of mTOR and loss of DEPTOR expression in glomerular mesangial cells results in mesangial cell hypertrophy (19, 20). In our 3g-treated mice, there was a similar effect in approximately 10% of glomeruli. Although there was no effect on renal function (normal BUN; Supplementary Fig. S6), we did not assay urine for protein urea and this will be addressed in future studies. Most renal expression of DEPTOR occurs in proximal tubular cells (ref. 24and Supplementary Fig. S7A) and tubular-specific deletion of DEPTOR did not alter renal histology or function (24).

Loss of DEPTOR expression with attendant enhanced mTOR activity in heart myocytes has been implicated in pathologic cardiac hypertrophy (21). Postmortem findings in drug 3g–treated immunocompetent mice confirmed cardiac DEPTOR loss, mTORC1 activation, and a modest increase in heart-to-tibia ratios. Although histologic examination of hearts did not confirm cardiac hypertrophy, the altered heart/tibia ratios are of concern. Interestingly, treatment of immunodeficient tumor-carrying mice (the experiment shown in Fig. 4C) did not demonstrate any cardiac enlargement (heart/tibia ratios were unaltered). This inconsistency may be due to the shorter duration of treatment (9 days instead of 21 days) or to a contribution of the immune system in development of cardiac hypertrophy. Nevertheless,

Published OnlineFirst August 8, 2019; DOI: 10.1158/1535-7163.MCT-19-0115

future lead compound optimization will address cardiac hypertrophy as a potential toxicity.

An additional concern was a moderate weight loss during treatment of mice with 20 mg/kg of drug (Fig. 4D). This corrected rapidly once treatment ceased. It is unclear if this represents an off-target side effect. High DEPTOR expression correlates with obesity (25) and protein levels of DEPTOR regulate adipogenesis by a cell-autonomous mechanism. Suppression of DEPTOR restricts the pro-adipogenic AKT/PPAR-γ axis through its effects on the mTORC1-mediated feedback loop (25). However, the rapidity of the weight loss and its resolution in our drug 3g-treated mice argue against this explanation. Nevertheless, it was gratifying that doses of 10 and 5 mg/kg did not result in any weight loss and yet induced significant anti-tumor effects in the SQ model (Supplementary Fig. S4A) and the marrow-based IV model (Fig. 4F). Additional experiments (Supplementary Fig. S5) demonstrate that loss of DEPTOR expression in tumors is still present by 48 hours postinjection of drug 3g and an every-other-day regimen is equally effective (versus daily treatment) against tumor outgrowth. Importantly, this comparable antitumor effect was not associated with any weight loss.

The results of Fig. 6 indicate DEPTOR expression can protect multiple myeloma cells against bortezomib. A similar protection occurs in multiple myeloma cells mediated by Che-1 gene expression (26), which may be due to ensuing Che-1-dependent DEPTOR expression (26). These results suggest that anti-DEPTOR drugs could synergize with PIs. Indeed, drug NSC126405 was significantly synergistic when combined with bortezomib (Fig. 6). The resulting mTOR activation and subsequent decreased autophagy is one potential mechanism for synergy as autophagy can regulate sensitivity to PIs in multiple myeloma cells (27, 28). However, combining bortezomib with drug 3g was not synergistic and, in fact, was antagonistic (CI = 1.8). The simple explanation for this result is that bortezomib prevented 3g-induced proteasomal degradation of DEPTOR and reversed part of 3g's anti-multiple myeloma effect. This potential antagonism is a caveat to future use of drug 3g in multiple myeloma if combined with PIs.

Disclosure of Potential Conflicts of Interest

No potential conflicts of interest were disclosed.

Authors' Contributions

Conception and design: P. Frost, S. Huerta-Yepez, J.F. Gera, A. Lichtenstein
Development of methodology: M.I. Vega, Y. Shi, P. Frost, S. Huerta-Yepez, M.E. Jung, J.F. Gera
Acquisition of data (provided animals, acquired and managed patients, provided facilities, etc.): M.I. Vega, Y. Shi, P. Frost, J. Lee, M.E. Jung
Analysis and interpretation of data (e.g., statistical analysis, biostatistics, computational analysis): M.I. Vega, S. Huerta-Yepez, G. Antonio-Andres, R. Hernandez-Pando, A. Lichtenstein
Writing, review, and/or revision of the manuscript: M.E. Jung, J.F. Gera, A. Lichtenstein
Administrative, technical, or material support (i.e., reporting or organizing data, constructing databases): M.E. Jung
Study supervision: A. Lichtenstein

Acknowledgments

The authors thank the UCLA Division of Laboratory Animal Medicine core service of the Jonsson Cancer Center for assessment of blood counts and liver function in injected mice. This work was supported by NIH grants RO1CA111448, RO1CA211562, R21CA168491, R01CA217820 and research funds of the VA and Multiple Myeloma Research Foundation.

The costs of publication of this article were defrayed in part by the payment of page charges. This article must therefore be hereby marked *advertisement* in accordance with 18 U.S.C. Section 1734 solely to indicate this fact.

Received January 31, 2019; revised June 19, 2019; accepted July 30, 2019; published first August 8, 2019.

References

1. Peterson TR, Laplante M, Thoreen CC, Sancak Y, Kang SA, Kuehl WM, et al. DEPTOR is an mTOR inhibitor frequently overexpressed in multiple myeloma cells and required for their survival. Cell 2009; 137:873–86.
2. Zhang HR, Chen JM, Zeng ZY, Que WZ. Knockdown of DEPTOR inhibits cell proliferation and increases chemosensitivity to melphalan in human multiple myeloma RPMI-826 cells via inhibiting PI3K/AKT activity. J Int Med Res 2013;41:584–95.
3. Shi Y, Daniels-Wells T, Frost P, Lee J, Finn RS, Bardeleben C, et al. Cytotoxic properties of a DEPTOR-mTOR inhibitor in multiple myeloma cells. Cancer Res 2016;76:5822–31.
4. Yang Y, Bardeleben C, Frost P, Hoang B, Shi Y, Finn R, et al. DEPTOR is linked to a TORC1-p21 survival/ proliferation pathway in multiple myeloma cells. Genes & Cancer 2014;5:407–19.
5. Benavides-Serrato A, Lee J, Holmes B, Landon KA, Bashir T, Jung ME, et al. Specific blockade of RICTOR-mTOR association inhibits mTORC2 activity and is cytotoxic in glioblastoma. PLoS One 2017;12;e0176599.
6. Holmes B, Lee J, Landon KA, Benavides-Serrato A, Bashir T, Junh ME, et al. Mechanistic target of rapamycin inhibition synergizes with reduced IRES-mediated translation of cyclin D1 and c-Myc mRNAs to treated glioblastoma. J Biol Chem 2016;291:14146–59.
7. Mysore VS, Szablowski J, Dervan PB, Frost PJ. A DNA-binding molecule targeting the adaptive hypoxic response in multiple myeloma has potent anti-tumor activity. Mol Cancer Res 2016;14:253–66.
8. Laurinaviciene A, Plancoulaine B, Baltrusaityte I, Meskauskas R, Besusparis J, Lesciute-Krilavicience D, et al. Digital immunohistochemistry platform for the staining variation monitoring based on integration of image and startistical analyses with laboratory information system. Diagnostoc Path 2014;9(Suppl 1):S10–S24.
9. Baay-Guzman G, Duran-Padilla MA, Rangel-Santiago J, Tirado-Rodriguez B, Antonio-andres G, Barrios-Payan J, et al. Dual role of hypoxia-inducible factor 1 alpha in experimental pulmonary tuberculosis: its implication as a new therapeutic target. Future Microbiol 2018;13:785–98.
10. Shi Y, Hoang B, Bardeleben C, Holmes B, Gera J, Lichtenstein A. Therapeutic potential of targeting IRES-dependent c-myc translation in multiple myeloma cells during ER stress. Oncogene 2016;35:1015–24.
11. Lee J, Shi Y, Vega M, Yang Y, Gera J, Jung ME, et al. Structure-activity relationship of small molecule inhibitors of the DEPTOR-mTOR interaction. Bioorg Med Chem Lett 2017; 27:4714–24.
12. O'Reilly KE, Rojo F, She QB, Solit D, Mills GB, Smith D, et al. mTOR inhibition induces upstream receptor tyrosine kinase signaling and activates AKT. Cancer Res 2006;66:1500–8.
13. Sun SY, Rosenberg LM, Wang X, Zhou Z, Yue P, Fu H, et al. Activation of AKT and eIF4E survival pathways by rapamycin-mediated mTOR inhibition. Cancer Res 2005;65:7052–8.
14. Gao D, Inuzuka H, Tan M-K, Fukushima H, Locasale JW, Liu P, et al. mTOR drives its own activation via $SCF^{\beta TrCP}$ -dependent degradation of the mTOR inhibitor DEPTOR. Molec Cell 2011;44:290–303.
15. Duan S, Skaar JR, Kuchay S, Toschi A, Kanarek N, Ben-Neriah Y, et al. mTOR generates an auto-amplification loop by triggering the betaTrCP- and CK1alpha-dependent degradation of DEPTOR. Mol Cell 2011;44:317–24.
16. Zhao Y, Xiong X, Sun Y. DEPTOR, an mTOR inhibitor, is a physiological substrate of SCF(betaTrCP) E3 ubiquitin ligase and regulates survival and autophagy. Mol Cell 2011;44:304–16.

Published OnlineFirst August 8, 2019; DOI: 10.1158/1535-7163.MCT-19-0115

17. Catena V, Bruno T, De Nicola F, Goeman F, Pallocca M, Iezzi S, et al. DEPTOR transcriptionally regulates endoplasmic reticulum homeostasis in multiple myeloma cells. Oncotarget 2016:7: 70546–58.
18. Betz C, Hall MN. Where is mTOR and what is it doing there? J Cell Biol 2013;203:563–74.
19. Das F, Ghosh-Choudhury N, Bera A, Dey N, Abboud HE, Kasinath S. TGF-beta integrates Smad 3 to mTOR complexes to arrest DEPTOR abundance for glomerular mesangial cell hypertrophy. J Biol Chem 2013;288: 7756–768.
20. Dey N, Ghosh-Choudhury N, Das F, Li X, Venkatesan B, Barnes JL, et al. PRAS40 acts as a nodal regulator of high glucose-induced TORC1 activation in glomerular mesangial cell hypertrophy. J Cell Physiol 2010;225: 27–41.
21. Gonzalez-Teran B, Lopez JA, Rodriguez E, Leiva L, Martinez-Martinez S, Bernal JA, et al. p38gamma and delta promote heart hypertrophy by targeting the mTOR-inhibitory protein DEPTOR for degradation. Nature Commun 2016;7:10477–87.
22. Quwaider D, Corchete LA, Misiewiez-Krzeminska I, Sarasquete M, Perez J, Krzeminski P, et al. DEPTOR maintains plasma cell differentiation and favorably affects prognosis in multiple myeloma. J Hemat Oncol 2017; 10: 92–104.
23. Caron A, Mouchiroud M, Gautier N, Labbe SM, Villot R, Turcotte L, et al. Loss of hepatic DEPTOR alters the metabolic transition to fasting. Molec Metab 2017;6:447–58.
24. Wang C, Dai H, Xiong Z, Song Q, Zou Z, Li M, et al. Loss of DEPTOR in renal tubules protects against cisplatin-induced acute kidney injury. Cell Death Dis 2018;9:441–52.
25. Laplante M, Horvat S, Festuccia WT, Birsoy K, Prevorsek Z, Efeyan A, et al. DEPTOR cell-autonomously promotes adipogenesis and its expression is associated with obesity. Cell Metab 2012;16:202–12.
26. Desantis A, Bruno T, Catena V, De Nicola F, Goeman F, Iezzi S, et al. Che-1-induced inhibition of mTOR pathway enables stress-induced autophagy. EMBO J 2015;34:1214–30.
27. Chang I, Wang CY. Inhibition of HDAC6 protein enhances bortezomib-induced apoptosis in head and neck SCC cancer by reducing autophagy. J Biol Chem 2016; 291:181990209.
28. Chen S, Zhang Y, Zhou L, Leng Y, Lin H, Kmiecak M, et al. A BIM-targeting strategy overcomes adaptive bortezomib resistance in myeloma through a novel link between autophagy and apoptosis. Blood 2014; 124:2687–97.

Published OnlineFirst August 8, 2019; DOI: 10.1158/1535-7163.MCT-19-0115

Molecular Cancer Therapeutics

A Novel Therapeutic Induces DEPTOR Degradation in Multiple Myeloma Cells with Resulting Tumor Cytotoxicity

Mario I. Vega, Yijiang Shi, Patrick Frost, et al.

Mol Cancer Ther 2019;18:1822-1831. Published OnlineFirst August 8, 2019.